


Medical Oncology (2018) 35:112  
<https://doi.org/10.1007/s12032-018-1170-z>

SHORT COMMUNICATION



## Simultaneous PET/MRI in assessing the response to chemo/radiotherapy in head and neck carcinoma: initial experience

Valeria Romeo<sup>1</sup>  · Brigida Iorio<sup>2</sup> · Massimo Mesolella<sup>2</sup> · Lorenzo Ugga<sup>1</sup> · Francesco Verde<sup>1</sup> · Emanuele Nicolai<sup>3</sup> · Mario Covello<sup>3</sup>

Received: 17 May 2018 / Accepted: 13 June 2018 / Published online: 19 June 2018  
 © Springer Science+Business Media, LLC, part of Springer Nature 2018

### Abstract

The purpose of the study was to assess by simultaneous positron emission tomography/magnetic resonance imaging (PET/MRI) the response to chemotherapy (CHT) and/or radiotherapy (RT) in patients with head and neck squamous cell carcinoma (HNSCC). Five patients with HNSCC underwent simultaneous PET/MRI examination before and after CHT and/or RT. Standard uptake volume (SUV), apparent diffusion coefficient (ADC), Ktrans, Kep, Ve, and iAUC pre- and post-treatment values were extracted and compared. The response to treatment was assessed according to RECIST criteria and classified as complete response (CR), partial response (PR), stable disease (SD), and progression disease (PD). In patient 1, PR was observed with increased ADC, Ktrans, and Ve values and reduction of SUV, iAUC, and Kep values; during clinical and instrumental follow-up, the patient experienced disease progression. Patient 2, classified as PR, showed increased ADC values and reduction of SUV and all perfusion parameters; follow-up demonstrated disease stability. Patient 3, considered as SD, showed increase of ADC and all perfusion values with a mild decrease of SUV; PD was observed during clinical and instrumental follow-up. Patients 4 and 5 showed a CR with no detectable tumor lesions at post-treatment PET/MRI examination, confirmed by 1-year follow-up. Multiparametric evaluation with simultaneous PET/MRI could be a useful tool to assess and predict the response to CHT and/or RT in patients with HNSCC.

**Keywords** Simultaneous PET/MRI · Head and neck cancer · Treatment response · Chemotherapy · Radiotherapy

✉ Valeria Romeo  
[valeria.romeo@unina.it](mailto:valeria.romeo@unina.it)

Brigida Iorio  
[brigida.iorio82@gmail.com](mailto:brigida.iorio82@gmail.com)

Massimo Mesolella  
[massimo.mesolella@unina.it](mailto:massimo.mesolella@unina.it)

Lorenzo Ugga  
[lorenzo.ugga@gmail.com](mailto:lorenzo.ugga@gmail.com)

Francesco Verde  
[francescoverde87@gmail.com](mailto:francescoverde87@gmail.com)

Emanuele Nicolai  
[e.nicolai@sdn-napoli.it](mailto:e.nicolai@sdn-napoli.it)

Mario Covello  
[echoplanare@gmail.com](mailto:echoplanare@gmail.com)

<sup>1</sup> Department of Advanced Biomedical Sciences, University of Naples Federico II, Via S. Pansini, 5, 80123 Naples, Italy

<sup>2</sup> Department of Neuroscience, Reproductive and Odontostomatologic Sciences, University of Naples Federico II, Naples, Italy

<sup>3</sup> IRCCS SDN, Naples, Italy

### Abbreviations

HNSCC	Head and neck squamous cell carcinoma
CHT	Chemotherapy
RT	Radiotherapy
PET/MRI	Positron emission tomography/magnetic resonance imaging
DWI	Diffusion-weighted imaging
DCE	Dynamic contrast enhanced
ADC	Apparent diffusion coefficient
CT	Computed tomography
FDG	Fluorodeoxyglucose
RT	Repetition time
TE	Echo time
TI	Inversion time
TIRM	Turbo inversion recovery magnitude
FSE	Fast spin echo
SPAIR	Spectral attenuated inversion recovery
FFE	Fast field echo
VIBE	Volumetric interpolated breath-hold examination
SUV	Standard uptake value

VOI	Volume of interest
MTV	Metabolic tumor volume
EES	Extravascular-extracellular space
iAUC	Initial area under the concentration curve
ROI	Region of interest
CR	Complete response
PR	Partial response
SD	Stable disease
PD	Progression disease
RECIST	Response evaluation criteria in solid tumors
HPV	Human papilloma virus
EBV	Epstein–Barr virus

## Introduction

Hybrid imaging with positron emission tomography/magnetic resonance imaging (PET/MRI) allows the simultaneous acquisition of quantitative PET and MRI data concerning biological processes [1]. A multiparametric approach to analyze pre-treatment diffusion-weighted imaging (DWI) and dynamic contrast-enhanced (DCE) MRI of primary tumors has the potential to predict treatment response to chemoradiation therapy in head and neck squamous cell carcinoma (HNSCC); particularly, Ktrans has been reported as a possible imaging biomarker in predicting the response to therapy in HNSCC [2, 3]. However, clinical thresholds and optimum methods for data acquisition and analysis have yet to be defined [4]. Moreover, PET/computed tomography (CT) has been shown to have a good diagnostic accuracy in the assessment of treatment response after chemotherapy (CHT) and/or radiotherapy (RT) for HNSCC with the potential to guide clinical decision-making [5]. Thus, a combined approach of PET and MRI may provide a better assessment of tumor microenvironment [6]. In this short report, we aimed to assess the response to CHT and/or RT in 5 patients with locally advanced HNSCC by extracting morphologic, metabolic and functional PET/MRI parameters and to possibly identify biomarkers predictive of the response.

## Materials and methods

Five consecutive patients (3 M, mean age:  $49 \pm 16.7$  years, range 28–76) with locally advanced, histologically proven HNSCC (2 hypopharynx carcinomas, 1 retromolar trigone carcinoma and 2 nasopharynx carcinomas) underwent contrast-enhanced PET/MRI of the head and neck region before and after CHT and/or RT. Clinical and histological data of each patient, including Human Papilloma Virus (HPV) and Epstein–Barr Virus (EBV) status for retromolar trigone and nasopharynx carcinomas respectively, are reported in Table 1. Post-treatment PET/MRI examinations were performed at least 3 months after treatment, while the clinical and instrumental follow-up was conducted for at least 1 year after treatment. The study was approved by our Institutional Review Board authorization and Ethical Committee “IRCCS Pascale” and written informed consent was obtained from all subjects.

### PET/MRI acquisition

2-(18F)fluoro-2-deoxy-d-glucose (2-(18F)FDG) PET/MRI was performed using a Biograph mMR (Siemens Healthcare, Erlangen, Germany). PET/MRI attenuation correction was obtained by means of 2-point Dixon 3-dimensional volumetric interpolated breath-hold T1-weighted MRI sequences, as previously described [7]. PET data acquisition occurred for the first 7 min during MR acquisition.

The MRI protocol was performed with a 16-channel head and neck coil, including axial Fast Spin Echo (FSE) T2-weighted, axial FSE T1-weighted and axial DWI, obtained with a single-shot echo planar 2d SPAIR sequence using three *b* values: 0, 500 and 800 s/mm<sup>2</sup>. Perfusion studies were obtained during intravenous administration of paramagnetic contrast agent (Magnevist, Bayer, Berlin, Germany) 0.2 ml/kg, with a flow rate of 3.5 ml/s, using a Volumetric interpolated breath-hold examination (VIBE) dynamic sequence with 50 measurements (time resolution: 6 s). Two pre-contrast axial VIBE sequences with variable flip angles were obtained for T1 mapping. Finally, axial isometric high-resolution VIBE and axial Fast Field

**Table 1** Patient population

Pt	Age	Location	TNM	Histology	Grade	HPV	EBV	Therapy
1	57	Hypopharynx	T4a N1 M0	Indifferentiate	G3	n.a.	n.a.	Concurrent CHT-RT
2	36	Hypopharynx	T4a N0 M0	SCC	G2	n.a.	n.a.	Concurrent CHT-RT
3	48	Retromolar trigone	T3 N2a M0	Indifferentiate	G3	–	n.a.	Concurrent CHT-RT
4	28	Nasopharynx	T4 N3a M0	Nonkeratinizing indifferentiate	G3	n.a.	+	Concurrent CHT-RT
5	76	Nasopharynx	T3 N0 M0	Nonkeratinizing indifferentiate	G3	n.a.	+	RT

SCC squamocellular carcinoma, HPV human papilloma virus, EBV Epstein–Barr virus, CHT chemotherapy, RT radiotherapy, n.a. not applicable

Echo (FFE) T1-weighted with fat-saturation sequences were acquired. The total MR acquisition time was about 30–40 min.

### Image analysis

A radiologist with 10 years of experience in head and neck imaging and a nuclear medicine specialist with 9 years of experience analyzed pre- and post-treatment PET/MRI images in consensus. The maximum SUV ( $SUV_{max}$ ) and metabolic tumor volume (MTV) with a threshold of 40% of the maximum signal intensity were calculated as previously performed [8]. Size, volume, structural features, and loco-regional infiltration of tumor lesions were assessed using both pre-contrast and high-resolution post-contrast images. The DCE-MRI images were post-processed as previously described [9, 10]. On the basis of Toft's model, the following parameters were calculated: transfer constant between vascular and extravascular-extracellular space (EES) (Ktrans); the volume of EES ( $V_e$ ); the transfer constant between EES and blood plasma (Kep); and the initial area under the concentration curve (iAUC) [11]. Free-hand ROI area values were positioned at the level of maximum lesion extension and then copied and pasted on each parametric map to extract Apparent Diffusion Coefficient (ADC), Ktrans, Kep, and iAUC mean values.

According to RECIST criteria, the response to treatment was classified as complete response (CR), partial response (PR), stable disease (SD), or progression disease (PD) [12]. The post-treatment evolution of morphological, functional, and metabolic parameters was assessed and integrated with clinical evaluation and follow-up conducted for at least 1 year after treatment.

### Results

A summary of all pre- and post-treatment PET/MRI parameters is reported in Table 2. In patient 1, classified as PR, a significant (> 30%) reduction of tumor size was observed; in this patient, there were also (a) reduction of  $SUV_{max}$ , iAUC, and Kep post-treatment values and (b) increase of ADC, Ktrans, and  $V_e$  post-treatment values; during clinical and instrumental follow-up, PD was observed and the patient died after 6 months. Patient 2, also classified as PR, showed a considerable reduction (> 30%) of tumor size; in this patient, an increase of ADC values and reduction of  $SUV_{max}$  as well as all perfusion post-treatment parameters was observed. Disease stability was confirmed during the follow-up. In patient 3, with a HPV-negative (HPV-) retromolar trigone carcinoma, a large intratumoral abscess was appreciable at first PET/MRI examination (Fig. 1); so that, in addition to CHT/

**Table 2** Pre- and post-treatment morphologic, metabolic, and functional data

Pt	Size (mm)	Volume (cm <sup>3</sup> )	$SUV_{max}$ 2D (bw)	$SUV_{max}$ 3D (bw)	MTV (cm <sup>3</sup> )	ADC (μm <sup>2</sup> /s)	iAUC <sub>mean</sub> (mM min) (×50)	Ktrans <sub>mean</sub> (min <sup>-1</sup> ) (×1000)	Kep <sub>mean</sub> (min <sup>-1</sup> ) (×100)	$V_e$ mean (×1000)	Clinical outcome
1 pre-treat	35 × 42	21.61	16.9	19	17.92	839.42 (679–1026)	963.3	116.89	37.66	296.72	PD
1 post-treat	23 × 30	13.25	9.84 (↓)	11.4 (↓)	13.07 (↓)	1193 (↑) (744–1708)	797.71 (↓)	179.52 (↑)	33.95 (↓)	503.18 (↑)	PD
2 pre-treat	43 × 30	16.6	11.5	14.4	14.87	1003 (741–1547)	1887.84	578.6	93.46	552.6	PR
2 post-treat	30 × 16	5.48	3.4 (↓)	3.08 (↓)	4.58 (↓)	1478 (↑) (854–2231)	387.08 (↓)	108.29 (↓)	16.58 (↓)	534.95 (↑)	PR
3 pre-treat	70 × 62	83.39	7.95	9.11	39.9	1085 (1004–1190)	616.88	106.36	25.42	387.11	PD
3 post-treat	50 × 40	67.23	6.95 (↓)	7.36 (↓)	22.87 (↓)	1273 (↑) (1063–1440)	732.59 (↑)	180.86 (↑)	61.41 (↑)	300.76 (↓)	PD
4 pre-treat	37 × 32	16.88	9.4	12.5	27.39	717 (566–850)	505.59	120.08	34.75	377.44	CR
4 post-treat*	–	–	2 (↓)	–	–	1757 (↑) (895–2211)	411 (↓)	92.14 (↓)	29.08 (↓)	330.67 (↓)	CR
5 pre-treat	32 × 18	7.66	11.4	12.4	5.21	715 (390–1413)	269.1	84.56	67.38	129.16	CR
5 post-treat	–	–	–	–	–	–	–	–	–	–	CR

\*Post-treatment functional measurements are referred to post-radiotherapy changes

Pre-treat pre-treatment, Post-treat post-treatment,  $SUV_{max}$  standard uptake value, MTV metabolic tumor volume, ADC apparent diffusion coefficient, iAUC initial area under the concentration curve

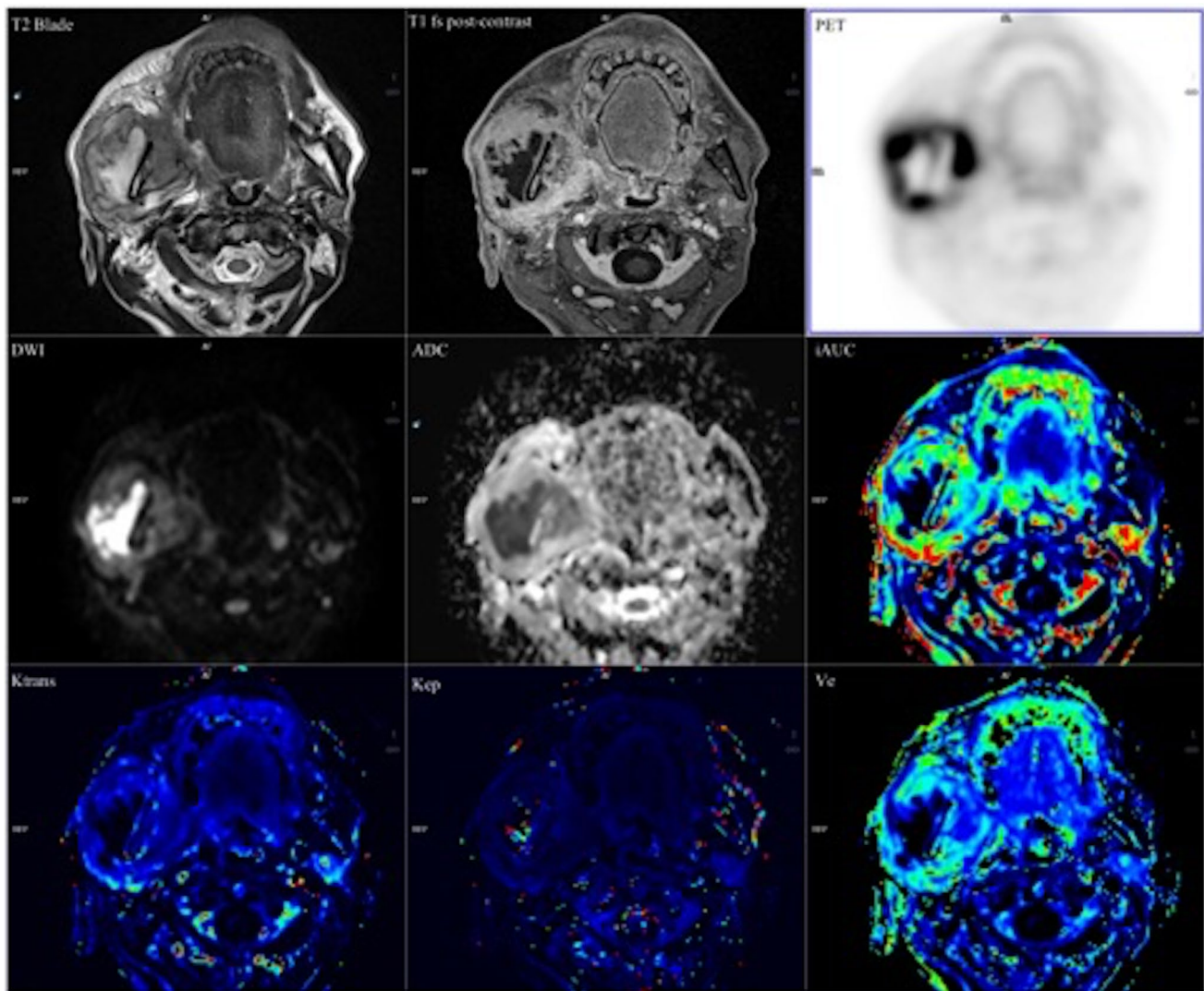


**Fig. 1** Multiparametric evaluation of morphological (TSE T2-weighted and contrast-enhanced FFE T1-weighted with fat saturation sequences), metabolic (PET) and functional (DWI, ADC, iAUC, Ktrans, Kep,  $V_e$ ) parameters in a 48-year-old female (patient 3) with

retromolar trigone carcinoma. The mass presents a central abscess as well as significant enhancement, high 2-(18F)FDG uptake, restricted diffusivity, and increased perfusion of the solid tumor tissue

RT, the patient underwent drainage of the purulent collection. Post-treatment PET/MRI examination demonstrated a reduction of the intratumoral abscess while the solid portion of the tumor remained substantially stable (Fig. 2); multiparametric analysis demonstrated an increase of ADC and all perfusion post-treatment values except for  $V_e$  and a mild (<30%) reduction of  $SUV_{max}$ . The response to treatment was initially considered as SD, but during the 1-year clinical and instrumental follow-up PD was observed. Both patients 4 and 5 with EBV-positive (HBV+) nasopharynx carcinoma showed a CR with no detectable tumor lesions on PET/MRI post-treatment examinations, also confirmed by 1-year follow-up. Of note, these two patients showed the lowest ADC and iAUC pre-treatment values.

## Discussion

Hypopharynx SCC frequently arises from pyriform sinus, posterior pharyngeal wall and postcricoid area [13]. Tumors are traditionally graded into well-, moderately, and poorly differentiated; TNM is the most significant predictor of survival [14, 15]. In our case series, the two patients with hypopharynx carcinoma initially showed a PR after concurrent CHT/RT according to RECIST criteria. However, while post-treatment changes in terms of lesion size, ADC, and some perfusion (iAUC and Kep) post-treatment values were similar in both cases, patient 1 showed a paradoxical increase of Ktrans and  $V_e$  values; moreover,  $SUV_{max}$  post-treatment values, even if significantly reduced in both cases, still

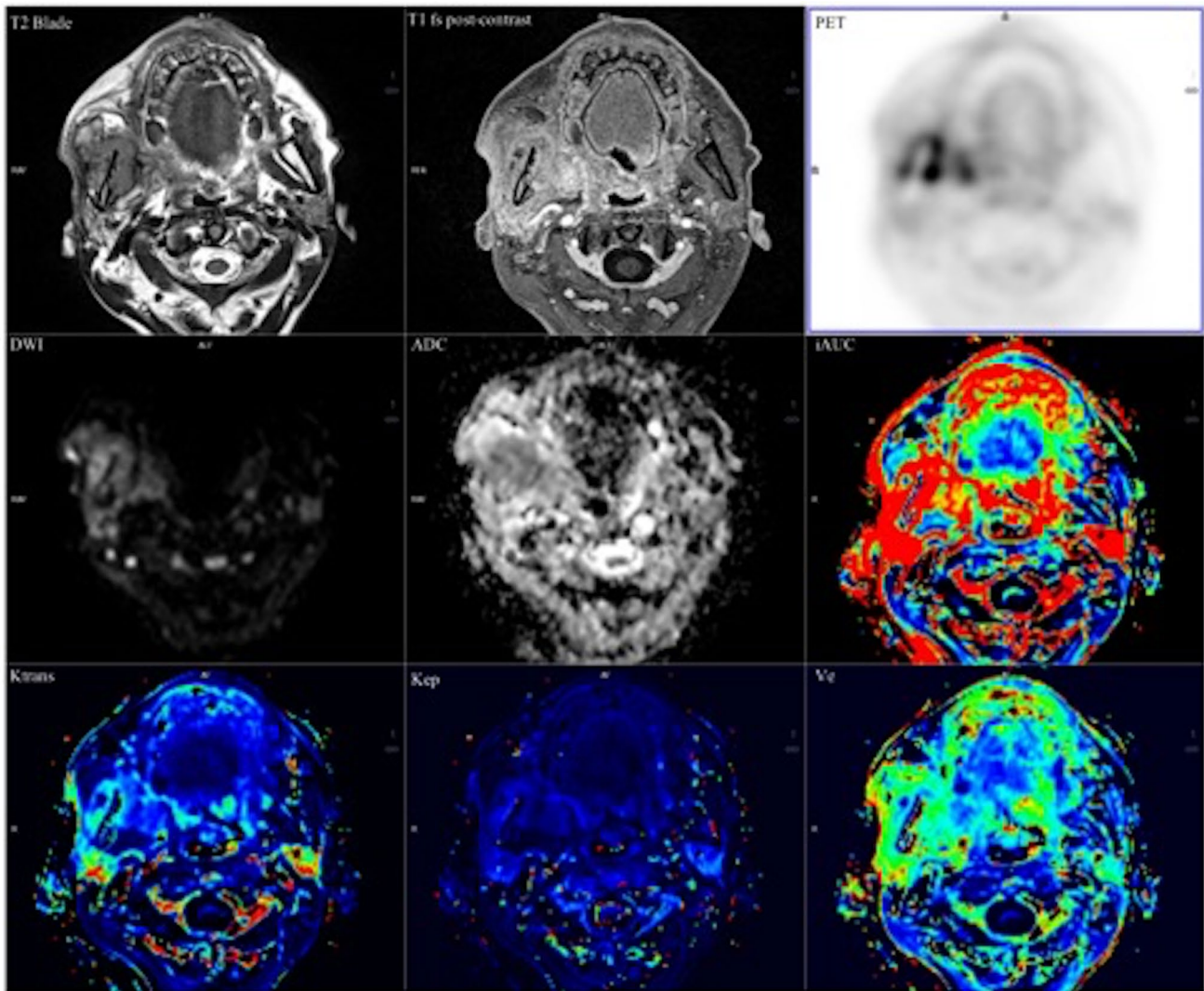


**Fig. 2** Multiparametric evaluation of morphological (TSE T2-weighted and contrast-enhanced FFE T1-weighted with fat saturation sequences), metabolic (PET) and functional (DWI, ADC, iAUC, Ktrans, Kep, V<sub>e</sub>) of the same patient reported in Fig. 1 (patient 3)

after chemo-radiotherapy and the drainage of the central abscess. A reduction of the purulent collection is appreciated while tumor extension, diffusivity, and perfusion are substantially stable with persistent high 2-(18F)FDG uptake

remained high (13.07) in patient 1 as compared to patient 2 (3.08). Differently from patient 2, patient 1 experienced disease progression during the clinical and instrumental follow-up and died after 6 months; in this setting, increased Ktrans and Kep as well as high SUV post-treatment values could be considered predictive of PD.

Cancer of the oral cavity represents one of the ten major causes of cancer death; HPV infection has been related to malignant tumors of the oropharyngeal–retromolar trigone region, together with other risk factors (e.g., smoking and alcohol) [16]. In our study, patient 3 with a HPV–retromolar trigone carcinoma, treated with concurrent CHT/RT, was initially classified as SD but experienced disease progression during the follow-up. Similar to patient 1, the increase of post-treatment perfusion parameters (iAUC, Ktrans, and

Kep) and high SUVmax post-treatment values could be considered predictive of PD, despite the stable lesion size.

Nasopharynx carcinoma is rare, near constantly associated with EBV infection, indicating a probable oncogenic role of this virus in the genesis of this tumor. The mainstay of treatment is radiation therapy and the presenting stage is the most important prognostic factor. Younger age and female gender are associated with better prognosis [17]. In our case series, both patients 4 and 5 with EBV+ nasopharynx carcinoma showed a CR with no detectable tumor lesions on PET/MRI post-treatment examinations. Interestingly, these two patients showed the lowest ADC pre-treatment values; this is in accordance with the current literature in which ADC values are reported as predictive of a good response to therapy [4]. Contrary to a recent

paper by Kim et al. in which high K<sub>trans</sub> pre-treatment levels were associated to a better response to therapy as compared to lower pre-treatment values [18], we found the lowest iAUC and K<sub>trans</sub> pre-treatment values in these two patients, supporting the hypothesis of a reduced aggressiveness of hypovascular tumors. However, this issue could be related to histological features of nasopharynx carcinoma and the difference could be explained by the lack of patients with nasopharynx carcinoma in their study. The role of DCE parameters in predicting and assessing the response to therapy in head and neck carcinoma is still discussed. In a previous study by King et al., who analyzed the role of DCE MRI for prediction and assessment of response to CHT and/or RT in patients with HNSCC, pre-treatment DCE-MRI did not predict which SCC sites would fail treatment, while site-control residual masses showed significantly lower reduction of K<sub>ep</sub> and iAUC values compared to site-failure residual masses [19]. In our case series, DCE parameters were useful to confirm the response to treatment according to morphological, metabolic, and diffusion data in patients with PR and CR and also aided, along with high SUV<sub>max</sub> post-treatment values, in identifying those patients, initially classified as PR or SD, who underwent disease progression during the clinical and instrumental follow-up.

In conclusion, according to our experience, multiparametric evaluation with contrast-enhanced simultaneous PET/MRI could be a useful tool to assess and predict the response to CHT and/or RT in patients with HNSCC. The comprehensive evaluation of tumor features provided by PET/MRI can aid in better assess the response to treatment and to identify patients at risk of disease progression. Additional studies in larger cohort of patients are necessary to confirm these data and to establish the role of PET/MRI in assessing and predict the response to treatment in head and neck cancer patients.

**Acknowledgements** This study was supported by Italian Ministry of Health for IRCCS SDN.

### Compliance with ethical standards

**Conflict of interest** The authors declare that they have no conflict of interest.

**Informed consent** Informed consent was obtained from all individual participants for whom identifying information included in this article.

**Research involving human participants and/or animals** All procedures performed in studies involving human participants were in accordance with the ethical standards of the institutional and/or national research committee and with the 1964 Helsinki declaration and its later amendments or comparable ethical standards.

### References

- Rosenkrantz AB, Friedman K, Chandarana H, et al. Current status of hybrid PET/MRI in oncologic imaging. *AJR Am J Roentgenol*. 2016;206:162–72.
- Chawla S, Kim S, Dougherty L, et al. Pretreatment diffusion-weighted and dynamic contrast-enhanced MRI for prediction of local treatment response in squamous cell carcinomas of the head and neck. *AJR Am J Roentgenol*. 2013;200:35–43.
- Kim S, Loevner LA, Quon H, et al. Prediction of response to chemoradiation therapy in squamous cell carcinomas of the head and neck using dynamic contrast-enhanced MR imaging. *AJNR Am J Neuroradiol*. 2010;31:262–8.
- King AD, Thoeny HC. Functional MRI for the prediction of treatment response in head and neck squamous cell carcinoma: potential and limitations. *Cancer Imaging*. 2016;16:23.
- Keski-Säntti H, Mustonen T, Schildt J, et al. FDG-PET/CT in the assessment of treatment response after oncologic treatment of head and neck squamous cell carcinoma. *Clin Med Insights Ear Nose Throat*. 2014;7:25–9.
- Jansen JF, et al. Noninvasive assessment of tumor microenvironment using dynamic contrast-enhanced magnetic resonance imaging and 18F-fluoromisonidazole positron emission tomography imaging in neck nodal metastases. *Int J Radiat Oncol Biol Phys*. 2010;77:1403–10.
- Eiber M, Martinez-Möller A, Souvatzoglou M, et al. Value of a Dixon-based MR/PET attenuation correction sequence for the localization and evaluation of PET-positive lesions. *Eur J Nucl Med Mol Imaging*. 2011;38:1691–701.
- Erdi YE, Mawlawi O, Larson SM, et al. Segmentation of lung lesion volume by adaptive positron emission tomography image thresholding. *Cancer*. 1997;80:2505–9.
- Covello M, Cavaliere C, Aiello M, et al. Simultaneous PET/MR head-neck cancer imaging: preliminary clinical experience and multiparametric evaluation. *Eur J Radiol*. 2015;84:1269–76.
- Cavaliere C, Romeo V, Aiello M, et al. Multiparametric evaluation by simultaneous PET-MRI examination in patients with histologically proven laryngeal cancer. *Eur J Radiol*. 2017;88:47–55.
- Tofts PS, Kermode AG. Measurement of the blood-brain barrier permeability and leakage space using dynamic MR imaging. 1. Fundamental concepts. *Magn Reson Med*. 1991;17:357–67.
- Eisenhauer EA, Therasse P, Bogaerts J, et al. New response evaluation criteria in solid tumours; Revised RECIST guideline (version 1.1). *Eur J Cancer*. 2009;45:228–47.
- Cattaruzza MS, Maisonneuve P, Boyle P. Epidemiology of laryngeal cancer. *Eur J Cancer B*. 1996;32:293–305.
- Cancer.gov [homepage on the Internet]. Hypopharyngeal cancer epidemiology and treatment; [updated 2016 december, 22]. [https://www.cancer.gov/types/head-and-neck/hp/adult/hypopharyngeal-treatment-pdq#link/\\_215\\_toc](https://www.cancer.gov/types/head-and-neck/hp/adult/hypopharyngeal-treatment-pdq#link/_215_toc). Accessed 3 Feb 2018.
- El-Naggar AK, Chan J, Takata T, Grandis J, Blootweg P. WHO classification of tumours. Pathology and genetics of head and neck tumours. 4th ed. Lyon: IARC Press; 2017.
- Horta R, Nascimento R, Silva A, Amarante J. The retromolar trigone: anatomy, cancer treatment modalities, reconstruction, and a classification system. *J Craniofac Surg*. 2016;27:1070–6.
- Chang ET, Adami HO. The enigmatic epidemiology of nasopharyngeal carcinoma. *Cancer Epidemiol Biomark Prev*. 2006;15:1765–77.
- Kim S, Loevner LA, Quon H, Poptani H, et al. Prediction of response to chemoradiation therapy in squamous cell carcinomas of the head and neck using dynamic contrast-enhanced MR imaging. *AJNR Am J Neuroradiol*. 2010;31:262–8.
- King AD, Chow SKK, Yu KH, et al. DCE-MRI for pre-treatment prediction and post-treatment assessment of treatment response in sites of squamous cell carcinoma in the head and neck. *PLoS ONE*. 2015;10(12):e0144770.